A high resolution millimetre and submillimetre study of W3

Astron. Astrophys. 221, 95–99 (1989)

ASTRONOMY AND ASTROPHYSICS

A high resolution millimetre and submillimetre study of W3

K.J. Richardson[1], G. Sandell[2], Glenn J. White[1], W.D. Duncan[2], and K. Krisciunas[2]

[1] Physics Department, Queen Mary College, University of London, Mile End Road, London E1 4NS, England
[2] Joint Astronomy Centre, 665 Komohana Street, Hilo, Hawaii, USA

Received November 21, 1988; accepted January 20, 1989

Summary. We have used the continuum bolometer receiver, UKT14, on the James Clerk Maxwell telescope to map the dense core of the star formation region W3 at wavelengths of 350, 800, and 1100 μm, with a spatial resolution of 15 to 20 arc sec. At 350 and 800 μm the region appears as two principal peaks around the known infrared sources IRS4 and IRS5, with each component having resolved structure. In addition, at 1100 μm, a further peak is apparent, not distinguishable at the other wavelengths, and interpreted as due to free-free emission around IRS2. This appears to be the most evolved H II region in the W3 Main complex, and is surprisingly free from surrounding dust. After allowing for the free-free contribution to the intensity, we find that the continuum dust emission from the region is consistent with optically thin emission at all 3 wavelengths, with the dust emissivity varying as λ^{-2} for wavelengths shortward of 800 μm. For wavelengths longer than this, a steeper variation is suggested by the data. Values for the dust optical depth, hydrogen column density, mass and central density are derived for each of the main peaks. Our mass estimates for the region are in good agreement with previous estimates from ^{13}CO observations and with dynamical models in which the region and its constituent components are in rotational/gravitational equilibrium.

Key words: H II regions – dust emission – molecular clouds – star formation

1. Introduction

W3 is a much studied site of active star formation which has been extensively observed in the near and far infrared (Wynn-Williams et al., 1972; Werner et al., 1980), in molecular lines (Dickel et al., 1980; Thronson, 1986) and at radio wavelengths (Wynn-Williams, 1971; Harris and Wynn-Williams, 1976; Colley, 1980; Roelfsema et al., 1987). Higher resolution has been obtained in molecular lines by aperture synthesis techniques (Claussen et al., 1984; Wright et al., 1984). High resolution single-dish observations have been obtained in millimetre molecular lines by Hayashi et al. (1989) and in the 4 and 6.5 mm continuum by Akabane et al. (1986).

The millimetre and submillimetre continuum is particularly useful for investigating a dense and highly obscured region such as this. For such wavelengths, the emission is likely to be optically thin and therefore to probe into the densest parts of the source; also, at wavelengths shortward of about 800 μm, the continuum is essentially dust emission which is largely uncontaminated by the free-free radiation from any associated ionised gas. This thermal radiation is relatively easy to interpret, compared with molecular line observations and shorter wavelength continuum radiation, both of which are likely to be subject to complex radiative transfer, scattering and extinction, while longer wavelength radio observations tend to probe the ionised or atomic components, which may account only for a small fraction of the mass of such regions. Furthermore, the millimetre and submillimetre emission usually falls in the Rayleigh-Jeans regime, so that the intensity is relatively insensitive to temperature, and the flux ratios at different wavelengths are temperature independent.

Previous mapping of W3 in this wavelength range has been carried out at 400 μm by Jaffe et al. (1987) and at 1.3 mm by Gordon and Jewell (1987), both at an angular resolution of about 30 arc sec. This present work represents a higher spatial resolution multi-wavelength study of this region, carried out with the newly operational James Clerk Maxwell Telescope[1].

2. Observations

The observations were carried out during the periods 28–29 August (350 μm) and 1–4 October (800 and 1100 μm) 1987, using the receiver UKT14 on the 15 m James Clerk Maxwell Telescope (JCMT), situated on the summit of Mauna Kea, Hawaii. The maps were made by dual beam mapping in Az-El, using a chop throw of 60 arc seconds, a step size of either 7.5 or 10 arc seconds, and a typical integration time per position of 5 seconds. The diffraction limited beamwidth (FWHM) at 1100 μm was 19 arc seconds, and this is also the resolution for our 800 μm map, though some mapping was also carried out at the diffraction limited resolution of 15 arc seconds. The aperture used at 350 μm was 15 arc seconds, but at this very early stage in the operating life of the antenna, there was a considerable error beam at this wavelength, of uncertain profile, but possibly containing up to 50% of the power, and which would have the effect of reducing the effective angular resolution at this wavelength. Since the

Send offprint requests to: K.J. Richardson

[1] The James Clerk Maxwell Telescope is operated on a joint basis between the United Kingdom Science and Engineering Research Council (SERC), the Netherlands Organisation for the Advancement of Pure Research (ZWO), the Canadian National Research Council (NRC), and the University of Hawaii (UH).

region is extended relative to the chop throw used, the area was covered by a raster scan in Az-El. The resultant dual beam maps were subsequently restored using the Emerson-Klein-Haslam algorithm (Emerson et al., 1979) with the "NOD2" software package (Haslam, 1974), which, suitably modified for the needs of the JCMT, was also used to correct the fluxes for atmospheric extinction, to calibrate them, and to convert the Az-El mapping into RA-dec maps.

Calibration was carried out on Uranus, Mars and Jupiter, with 3C84, W75N and W3(OH) being used as secondary calibrators. From calibration on the 50 arc sec disc of Jupiter, we estimate that the conversion factor from Jy/steradian to Jy/beam is $6.0\ 10^{-9}$ for the 15 arc sec resolution data and $8.9\ 10^{-9}$ for 19 arc sec resolution. For the 350 μm data, this would not adequately take into account any portion of the error beam which fell outside the Jovian disk. The measured fluxes for the compact H II region W3(OH) were 12 ± 0.3Jy (1100 μm, 19 arc sec beam), 32.6 ± 1.5Jy (800 μm, 19 arc sec beam) and 24.3 ± 1.3Jy (800 μm, 15 arc sec beam). The pointing was also checked on these objects, and is believed to be correct to 2–3 arc sec within a map, though somewhat larger absolute pointing errors (e.g. 5 arc sec) are possible.

The atmospheric conditions for the 800 and 1100 μm observations were worse than average for Mauna Kea; typical zenith sky opacities were 0.4 during the 1100 μm observations and 1.0 for the 800 μm data. For the 350 μm observations (29 August), the sky was excellent, with a zenith optical depth of ~ 0.6. The relative calibration within a wavelength band is estimated to be correct to within 10%, but the absolute calibration may be subject to larger errors; possibly 15% at 1100 μm, 20% at 800 μm and up to a factor of 2 at 350 μm.

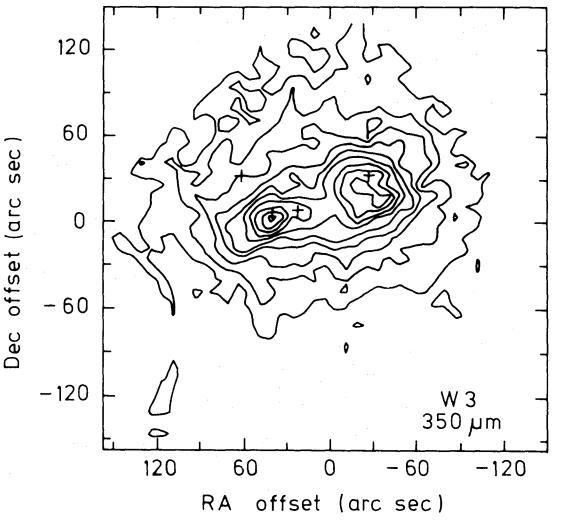

Fig. 1. Map of W 3 at 350 μm. Map size 5×5 arc min. Positions are offsets in arc sec from the map reference position. α(1950) 02 21 47.3; δ(1950) 61 52 15. On the map are also marked the positions (from left to right) of:

IRS2 α(1950) 02 21 56.8, δ(1950) 61 52 42;
IRS5 α(1950) 02 21 53.2, δ(1950) 61 52 21;
IRS3 α(1950) 02 21 50.3, δ(1950) 61 52 22;
IRS4 α(1950) 02 21 43.5, δ(1950) 61 52 49.

Contour levels in intervals of 20 Jy/beam, starting at 20. Beamwidth (FWHM) 15 arc sec

3. Morphology

The maps of W3 at 350, 800 and 1100 μm are shown in Figs. 1, 2 and 3, with the positions of the near infrared sources IRS2, IRS5, IRS3 and IRS4 (Wynn-Williams et al., 1972) superimposed.

The basic double peaked structure seen at 400 μm by Jaffe et al. (1983), and at 50 and 100 μm by Werner et al. (1980), and corresponding approximately in position with IRS5 and IRS4, is also apparent in our maps. In the 50 and 100 μm maps by Werner et al. (1980), the Western peak (IRS4) has less than half the intensity of the Eastern (IRS5). However, at 350 and 800 μm, the Western component has become relatively more prominent and the intensities and fluxes of the two components are roughly similar.

Our mapping reveals structure not resolved in the previous continuum studies at these wavelengths. At all three wavelengths, the IRS5 source is extended along the East-West direction, and to the West a subsidiary peak corresponding in position to IRS3 is becoming apparent. This is also seen in the 4 mm map by Akabane et al. (1986). The submillimetre emission also clearly peaks South of IRS4 which (especially at 800 and 1100 μm) has a distinctly triangular shape. This is most clearly seen in the 800 μm map, where there is a NE-SW extension in the emission around IRS4 (possibly due to two separate partially resolved peaks) and another peak about 20 arc sec to the south. Despite the relatively poor signal to noise on our 800 μm map, we believe these features to be real, since they were seen in two separate maps taken on different nights, one of which was at the diffraction limited

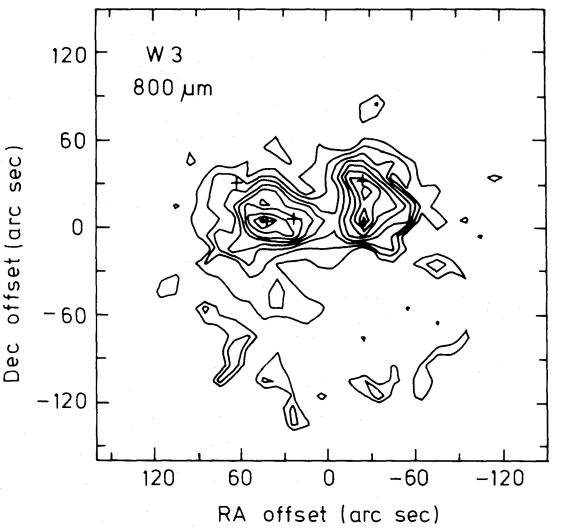

Fig. 2. 800 μm. Contour interval 1.5 Jy/beam, starting at 3.0. Beamwidth 19 arc sec. Otherwise same as Fig. 1

angular resolution of 15 arc sec. (Fig. 2 is a coaddition of these two maps, both converted to the same effective beam size of 19 arc sec.) A similar morphology is seen also at 350 μm, though here the effective resolution is likely to have been considerably degraded from the nominal 15 arc sec because of the error beam.

Perhaps the most striking difference between the maps of W3 is the extra emission peak seen to the NE of IRS5 at 1100 μm. This

Table 1. Source fluxes and peak intensities. Regions X, Y and Z are shown in Fig. 1. Errors in fluxes are dominated by calibration rather than statistical errors (see Sect. 2)

Region	1100 μm				800 μm				350 μm			
	Peak int. (GJy sr^{-1})	Flux (Jy)	Free free (Jy)	Dust (Jy)	Peak int. (GJy sr^{-1})	Flux (Jy)	Free free (Jy)	Dust (Jy)	Peak int. (GJy sr^{-1})	Flux (Jy)	Free free (Jy)	Dust (Jy)
X	0.57	38	21	17	—	62	20	42	—	1460	19	1440
Y	0.71	20	5.6	15	1.8	160	5.4	155	34.8	2400	5.0	2400
Z	0.48	56	1.9	55	1.7	266	1.8	264	32.5	5200	1.7	5200
Total	—	115	28	87	—	488	27	460	—	9000	25	8970

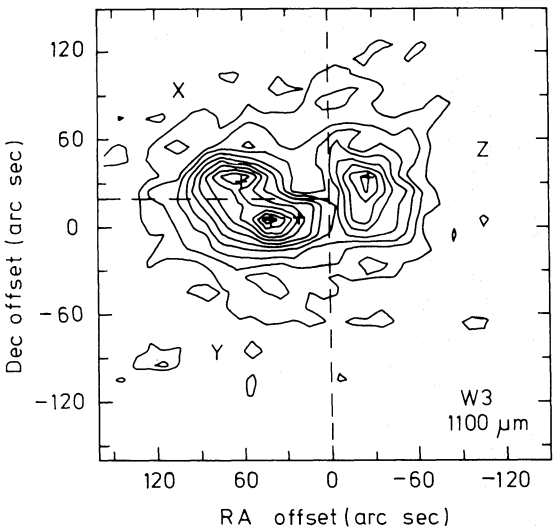

Fig. 3. 1100 μm. Contour interval 0.25 Jy/beam, starting at 0.25. Beamwidth 19 arc sec. The extents of regions X, Y and Z are shown. Otherwise same as Fig. 1

surrounds IRS2, and is approximately coextensive with the 6 cm radio emission first observed by Wynn-Williams et al. (1971). The 1.3 mm map by Gordon and Jewell (1987) shows only a single source corresponding to the IRS2–IRS5 region, but the higher angular resolution of the present observations resolves it into two distinct sources. The extra 1100 feature is readily interpreted as due to free-free emission with hardly any contamination from dust. It is not seen in our 800 μm map, because it does not go as deep as our 1.1 mm map.

In Table 1 we give the integrated fluxes at each wavelength for each of the 3 subregions shown in Fig. 3, together with the peak intensities. In addition we have attempted to subtract off the contributions due to free-free emission, by extrapolation from the 6 cm fluxes measured by Wynn-Williams et al. (1971).

4. Results

As mentioned in the Introduction, the radiation in this wavelength range is thought to be optically thin and to lie in the Rayleigh Jeans regime. The justification usually given for this rests on determinations of the temperature made at shorter wavelengths. When reasonably complete photometry is available, one can attempt to fit the data by a black body curve multiplied by an assumed functional form for the dust emissivity variation, commonly assumed to be a power law (e.g. see Richardson et al., 1985; Gordon, 1987). When such an analysis is carried out, it is invariably found that the absolute intensity over the submillimetre range is only a small fraction of that which would be given by an opaque black body at the derived temperature; this ratio (in conjunction with any appropriate geometrical factors to account for the source and beam sizes) gives the optical depth. However, such a procedure is of dubious validity if, as may well be the case, there are localised heat sources either inside or outside the cloud, with associated temperature gradients. The optical depths for the wavelengths which largely determine the derived temperature value may exceed unity, and the data at the different wavelengths may in fact be sampling different depths within the cloud. Apart from the uncertainty in the temperature, it is also possible that the absolute submillimetre flux falls below the black body value, not because it is optically thin, but because in an inhomogeneous region the emission may come from clumps much smaller than the beam and thus be beam-diluted.

However, with the current data we have an independent check on the optically thin assumption. Under optically thin conditions, and a $\lambda^{-\beta}$ emissivity variation, the ratio of fluxes at two wavelengths is given by

$$R_{\lambda_1,\lambda_2} \equiv \left(\frac{\lambda_2}{\lambda_1}\right)^{3+\beta} \frac{\exp\left(\frac{hc}{\lambda_2 kT}\right)-1}{\exp\left(\frac{hc}{\lambda_1 kT}\right)-1} \quad (1)$$

assuming equal beamwidths at the two wavelengths. In the Rayleigh Jeans regime, the last term in Eq. (1) reduces to the ratio of wavelengths. This occurs (to within an error of 10%) at temperatures >27 K, for $R_{800,1100}$; and temperatures >95 K, for $R_{350,800}$. Any positions of high dust optical depth, or of departure from the Rayleigh Jeans regime should be apparent from a variation in R_{λ_1,λ_2} across the source. However, from Table 2, in which the various ratios are given for both peak and integrated intensities, we see that no such significant variation occurs in $R_{350,800}$, whose value remains in the range 19.5 ± 0.5. This is the case whether one uses the integrated emission over regions X–Y and Z, or the peak intensities. For the ratio $R_{800,1100}$ the situation is not so clear; however the value of this ratio is more sensitive to the estimate of the free-free component to be subtracted off. Since

Table 2. Flux ratios for dust emission. "Total" values are ratios of integrated intensities over each region

	Observed				Theoretical		
	Region X/Y		Region Z		$\beta=1$	$\beta=2$	$\beta=3$
	Peak	Total	Peak	Total			
350/800	20.0	19.5	19.1	19.7	9.7	22.5	52.1
800/1100	2.8	6.2	3.5	4.8	2.6	3.4	4.6

Table 3. Derived source parameters from 800 μm observations. Assumes $T_{dust}=65$ K; $\beta=2$

Region	τ_{800} (peak)	N_{H_2} (peak) (10^{23} cm^{-2})	n_{H_2} (peak) (10^5 cm^{-3})	Mass ($M_\odot$)
X/Y	$7.4\ 10^{-3}$	2.1	1.0	1520
Z	$7.0\ 10^{-3}$	2.0	0.9	2040
Total	—	—	—	3600

in any case both a high optical depth and departure from the Rayleigh Jeans regime would occur first at 350 μm and since the shorter wavelengths are least prone to free-free contamination, we therefore conclude that the dust emission at all three wavelengths is optically thin, a conclusion which is independent of the absolute calibration.

The absolute value of R_{λ_1,λ_2} can be used to estimate the index of dust emissivity variation, β. One situation which may hinder a simple determination of β in this way is where temperature or (more importantly) density gradients are present in the region (e.g. see Emerson, 1988), as indeed they are in this case. It is then possible that the spectral index of the source can be modified due to the superposition of a range of different black body curves originating from different points across the region. But, as also pointed out by Emerson (1988), this complicating effect only occurs for the frequency range over which the modified black body curve peaks for the range of temperatures within the source. For it to be important at e.g. 350 μm would require the presence of an appreciable amount of gas at temperatures of ≤ 20 K. Since estimates of dust temperatures within W 3 range typically from 50–100 K (Gordon, 1987; Werner et al., 1980), we will neglect such effects here. (We note, however, that Akabane et al., 1986, did postulate the existence of a cold component to the dust emission, in order to fit the 4 mm emission. This they interpreted as originating from interstellar "stones" of several millimetres in size and at a temperature of 7 K.) The constancy of $R_{350,800}$ across the region suggests that no change in β occurs across the region between these two wavelengths, and its absolute value indicates a λ^{-2} variation.

The value of $R_{800,1100}$ for the peak fluxes in region Z (IRS4) also imply $\beta=2$. However, for the ratios from the integrated fluxes, larger values are suggested, i.e. 3.2 for region Z, and 4.1 for region X–Y, though for the latter, the data are severely contaminated by the free-free component. By using these values of β, correcting for the difference in effective wavelength and adding our estimate of the free-free contribution, our data would predict total 1.3 mm fluxes of 38 Jy for region X–Y and 24 Jy for region Z. These are consistent, within the likely errors, with the measured values of 28 and 18 Jy (Gordon and Jewell, 1987). It seems then that the dust emissivity variation longward of 800 μm is actually steeper than $\beta=2$.

In using our data to estimate optical depths, gas column densities and cloud masses, we will use the simplest possible interpretation of the observations which are consistent with the likely errors. We will assume that the emission is everywhere optically thin at a constant temperature of 65 K (Gordon, 1987) and that the dust has a constant β value of 2. We will initially use the 800 μm data because of the antenna error beam at 350 μm and the free-free contamination at 1100 μm.

For the average optical depth within the beam, we have

$$\tau=\frac{(\lambda/\mathrm{cm})^3}{2ch}\left(\exp\left(\frac{hc}{\lambda kT}\right)-1\right)S_\nu(\mathrm{Jy/sterad})\ 10^{-23} \quad (2)$$

An estimate of the gas column density is given (Hildebrand, 1983) by $N_{H_2}=2.8\ 10^{25}\tau_{800}$ [cm^{-2}]. Values for these quantities, together with estimates of the central gas densities of the IRS4 and IRS5 cores (assuming Gaussian density distributions) and total gas masses, are given in Table 3. These indicate peak 800 μm optical depths of $\simeq 0.007$ (and hence 350 μm optical depths of $\simeq 0.04$), confirming the conclusion of low optical depths from the flux ratios. Central peak densities are estimated to be $n_{H_2}\simeq 10^5$ cm^{-3}, though higher values are of course possible if there is even smaller scale structure within the cores, which indeed our observations show to be present. Our estimate of the total mass of the region is $\simeq 3600\ M_\odot$, though if we use the 1100 μm or 350 μm fluxes, together with an assumed $\beta=2$, we obtain $\simeq 2200\ M_\odot$ and $\simeq 2900\ M_\odot$ respectively. By contrast, Jaffe et al. (1983) estimated $\simeq 900\ M_\odot$ for the region. Our estimates of the total mass, as well as those of the two main clumps, are however very similar to those estimated by Hayashi et al. (1989) from ^{13}CO line observations.

One particularly significant point of agreement with the last named authors is that the condensation of gas surrounding IRS4 (i.e. region Z) is significantly more massive than that surrounding IRS5 (region X–Y). Region X–Y however exhibits to a much greater extent the energetic activity associated with star formation e.g. relatively luminous H II regions around IRS2 and IRS3 (e.g. Roelfsema et al., 1987) and an outflow associated with IRS5 (Claussen et al., 1984). Region Z, and especially the region immediately south of IRS4 (which itself has an associated H II region) is much more quiescent, and it seems plausible that the material here represents an earlier stage in the star formation process.

Though the closeness of the agreement between the mass estimates from the present data and those made by Hayashi et al. (1989) is probably fortuitous, it is nonetheless interesting that the submillimetre continuum estimates agree with the results from molecular line observations. Typical time scales for the condensation of molecules onto dust grains are $\simeq 10^9/n_{H_2}$ years (Williams, 1986), so in such dense and clumpy regions as W 3, one might expect to have enormous fluctuations in abundances from point to point. In fact, this seems to be borne out by the high resolution maps currently available. For example, Wright et al. (1984) detected HCN emission around IRS4, but none around IRS5 (see also the HCO^+ mapping by Hayashi et al., 1989). These molecules are often cited as a probe of high densities, but it would

seem that here there are other e.g. abundance and/or radiative transfer factors, which swamp the density effect. The ^{13}CO $J=1$–0 line is more likely than HCN $J=1$–0 to be optically thin; however in the CO mapping by Hayashi et al. (1989), the authors note the presence of a wide variety of velocity components, which appear and disappear from point to point, and do not in general coincide with known infrared sources. Such line observations are indispensible in investigating the kinematical morphology and the chemical composition of cloud cores, but cannot be assumed a priori to be reliable mass tracers. Now that submillimetre continuum mapping at several wavelengths is possible, we have a powerful independent technique both for checking whether emission is optically thin, and for probing gas densities.

5. Conclusions

We have mapped the central region of the W3 molecular cloud at wavelengths of 350, 800 amd 1100 μm, using the James Clerk Maxwell Telescope. At all three wavelengths, the double peaked structure of the source is seen, with condensations of mass around the infrared peaks IRS4 and IRS5. In addition, a third peak is seen at 1100 μm, corresponding to free-free emission around IRS2. Also, there are indications at all three wavelengths of smaller scale structure within each of the main peaks, which future observations at an angular resolution of 15 arc sec or better will be able resolve unambiguously. From the absolute fluxes and the flux ratios, we deduce that the dust emission is optically thin at all three wavelengths and that gas densities $\geq 10^5$ molecules cm^{-3} are present in the dense cores. Our estimates of the mass structure of the region are consistent with those from the recent ^{13}CO line observations of Hayashi et al. (1989) using similar angular resolution, and hence with their interpretation of the dynamics of the region. Such mapping in the millimetre and submillimetre continuum provides a powerful and unambiguous probe of the density structure of such dense and inhomogeneous regions as these, which is independent of complex radiative transfer and chemical abundance variations.

Acknowledgements. We thank the staff of the Joint Astronomy Centre, Hilo for operation of and assistance at the telescope; in particular, Saeko Hayashi, Iain Coulson and Sheldon Remington. KJR and GJW also acknowledge the support of the SERC for travel grants and the funding of millimetre and submillimetre astronomy in the UK.

References

Akabane, K., Hirabayashi, H., Sofue, Y.: 1986, *Pub. Astron. Soc. Japan*, **38**, 77

Claussen, M.J., Berge, G.L., Heiligman, G.M., Leighton, R.B., Lo, K.Y., Masson, C.R., Moffet, A.T., Phillips, T.G., Sargent, A.I., Scott, S.L., Wannier, P.G., Woody, D.P.: 1984, *Astrophys. J.*, **285**, L79

Colley, D.: 1980, *Monthly Notices Roy. Astron. Soc.* **193**, 495

Dickel, H.R.: 1980, *Astrophys. J.* **238**, 829

Dickel, H.R., Dickel, J.R., Wilson, W.J., Werner, M.W.: 1980, *Astrophys. J.* **237**, 711

Emerson, D.T., Klein, U., Haslam, C.G.T.: 1979, *Astron. Astrophys.* **76**, 92

Emerson, J.P.: 1988, in *Formation and Evolution of Low Mass Stars, Proc.* NATO Advanced Study Institute, Viano do Castelo, Ed. A.K., Dupree, M.T.V.T. Lago, Reidel

Gordon, M.A.: 1987, *Astrophys. J.* **316**, 258

Gordon, M.A., Jewell, P.R.: 1987, *Astrophys. J.* **323**, 766

Harris, S., Wynn-Williams, C.G.: 1976, *Monthly Notices Roy. Astron. Soc.* **174**, 649

Haslam, C.G.T.: 1974, *Astron. Astrophys. Supl.* **15**, 333

Hayashi, M., Kobayashi, H., Hasegawa, T.: 1988, *Astrophys. J.* **340**, 298

Hildebrand, R.H.: 1983, *Q. Jl. Roy. Astron. Soc.* **24**, 267

Jaffe, D.T., Hildebrand, R.H., Keene, J., Whitcomb, S.E.: 1983, *Astrophys. J.* **273**, L89

Roelfsema, P.R., Goss, W.M., Wilson, T.L.: 1987, *Astron. Astrophys.*, **174**, 232

Richardson, K.J., White, G.J., Gee, G., Griffin, M.J., Cunningham, C.T., Ade, P.A.R.: 1985, *Monthly Notices Roy. Astron. Soc.* **216**, 713

Thronson, H.A.: 1986, *Astrophys. J.*, **306**, 160

Williams, D.A.: 1986, *Q. Jl. Roy. Astron. Soc.* **27**, 64

Werner, M.W., Becklin, E.E., Gatley, I., Neugebauer, G., Sellgren, K., Thronson, H.A., Harper, D.A., Loewenstein, R., Moseley, S.H.: 1980, *Astrophys. J.* **242**, 601

Wright, M.C.H., Dickel, H.R., Ho, P.T.P.: 1984, *Astrophys. J.* **281**, L71

Wynn-Williams, C.G.: 1971, *Monthly Notices Roy. Astron. Soc.* **151**, 397

Wynn-Williams, C.G., Becklin, E.E., Neugebauer, G.: 1972, *Monthly Notices Roy. Astron. Soc.* **131**, 159